IOSR Journal of Applied Physics (IOSR-JAP)
e-ISSN: 2278-4861.Volume 6, Issue 2 Ver. III (Mar-Apr. 2014), PP 58-65
www.iosrjournals.org

Influence of Zn substitution on the structural and magnetic properties of $Co_{1-x}Zn_xFe_2O_4$ nano-ferrites

S. Nasrin[1*], S. Manjura Hoque[2], F.-U.-Z Chowdhury[3], M. Moazzam Hossen[4]
[1]*Department of Physics, University of Chittagong, Chittagong, Bangladesh. shamima.physics@cu.ac.bd*
[2]*Materials Science Division, Atomic Energy Centre, Dhaka, Bangladesh.*
[3]*Department of Physics, Chittagong University of Engineering & Technology, Chittagong, Bangladesh.*
[4]*Department of Computer Science & Engineering, International Islamic University Chittagong, Chittagong, Bangladesh.*

Abstract: *Polycrystalline samples of $Co_{1-x}Zn_xFe_2O_4$ with stoichiometric proportion (x) varying from 0.2 to 0.8 were prepared through the wet chemical co-precipitation method. The samples were sintered at 200ºC and 400ºC for 3 h and characterized using X-ray diffraction (XRD) technique. XRD studies revealed the formation of single phase spinel cubical structure. The values of lattice constant, grain size, X-ray density, bulk density, porosity, ionic radii, bond length and hoping length of tetrahedral and octahedral sites have been calculated using X-ray diffraction data. The lattice constant has been found to be increases after sintering the sample at 400ºC. The magnetic properties such as the low field hysteresis loop, magnetization versus temperature curve, saturation magnetization, remanent magnetization, coercivity, Y-K angle and Curie temperature have been determined by using vibrating sample magnetometer (VSM) data. The value of coercivity confirmed that soft ferrites have been obtained. The value of Curie temperature has been found to be increases with the increase of sintering temperature, while the value of Curie temperature decreases with the increase of Zn content.*

Key words: *Coercivity; Saturation magnetization; Spinel ferrites; VSM; X-ray diffraction; Y-K angle.*

I. Introduction

Ferrites continue to be a fascinating magnetic material because of their potential applications in high density information, ferro-fluids, magnetic resonance imaging, biomedical diagnostics, drug delivery, high frequency electronic devices, sensors, permanent magnets and magnetic refrigeration system etc [1-5]. The magnetic properties of ferrite materials strongly depend on their chemical compositions and substitutions. A small amount of foreign ions in the ferrite can dramatically change the properties of ferrites. The magnetic properties of Zn-substituted Co-ferrites have attracted considerable attention because of the importance of these materials for data storage applications. $CoFe_2O_4$ has inverse spinel structure with Co^{2+} ions in octahedral sites and Fe^{3+} ions equally distributed between tetrahedral and octahedral sites whereas $ZnFe_2O_4$ has a normal spinel structure with Zn^{2+} ions in tetrahedral and Fe^{3+} in octahedral sites [6]. Therefore, Zn-substitution in $CoFe_2O_4$ may have some distorted spinel structures depending upon the concentration of the precursor solutions. Magnetic properties of spinel ferrites are also influenced by morphology, especially by their crystallite size; hence, in biomedical and modern data storage application it is important to control the particles morphology [7]. Dey and Ghose prepared $Co_{0.2}Zn_{0.8}Fe_2O_4$ by co-precipitation method and found decrease in magnetization with increasing particle size [8]. Arulmurugan et al. [9] suggested that substitution of Co^{2+} with Zn^{2+} lead to improved magnetic properties of nanocrystalline ferrites. They also observed a decreasing behaviour of saturation magnetization and the particle size of the Co-Zn substituted ferrite nano-ferrites with increasing Zn concentration. Islam et al. [10] reported that saturation magnetization decreases with zinc concentration in cobalt zinc ferrites prepared by ceramic technique. Vaidyanathan et al. [11] also reported decrease in magnetic properties such as M_S, H_S, H_C and M_r with increase in zinc substitution.

The present work deals with the synthesis of nano particles of zinc substituted cobalt ferrite ($Co_{1-x}Zn_xFe_2O_4$ where $x= 0.2, 0.4, 0.6$ and 0.8) via wet co-precipitation method and characterized using X-ray diffractometry (*XRD*) and vibrating sample magnetometer (*VSM*). Studies were also carried out after sintering the sample at 200ºC and 400ºC to see the effect of grain size, lattice constant and other structural parameters on magnetic properties. This work is an attempt to on the influence of Zn substitution on the structural and magnetic properties of zinc substituted cobalt nano-ferrites.

II. Experimental

2.1 Sample Preparation

$Co_{1-x}Zn_xFe_2O_4$ nano-ferrites have been prepared by wet chemical co-precipitation method. In order to prepare the nano-ferrites through co-precipitation method required molar ratio in the stoichiometric range of

[M]:[Fe]⇒1:2 of relevant salts were dissolved in distilled water. The salts used in this study for the preparation of different ferrites are $CoCl_2.6H_2O$, $Zn(NO_3).6H_2O$ and $FeCl_3$. Sodium hydroxide (*NaOH*) was used as the co-precipitating agent. The salt solutions were added into the *8M* of *NaOH* solution with continuous stirring. *NaOH* was added to maintain *pH* of the solution to a value of 11 and allowed to react for 30-40 minute. In order to complete the ferritization reaction of Co based ferrites the particles were heated at 90ºC for 60 minute. Ferritization reaction of Fe_2O_4 has been carried out at room temperature to avoid oxidation. The precipitate was collected through centrifugation at 8000 rpm for 15 minute followed by rigorous washing through filtration. The calcined powders were then pressed uniaxially into disk-shaped (about 7.6-8.1 mm diameter, 0.9-1.0 mm thickness) samples. The samples were sintered at 200ºC and 400ºC in air for three hour. The temperature ramp was 7ºC/min for heating.

2.2 Measurements

The single phase ferrite formation of sintered powder was confirmed by powder *XRD* technique using X ray diffractometer with Cu-K_α radiation (λ= 1.54 Å). For each sample a scan has been performed from 25º to 70º with a step size of 0.02º. Magnetic measurements for samples in the same composition range have been done by using Vibrating Sample Magnetometer (*VSM*).

The bulk density, ρ_b was determined using the formula

$\rho_b = \frac{m}{\pi r^2 h}$, where *m* is the mass, *r* the radius and *h* the height of the sample.

The X-ray density, ρ_x was calculated using the relation [12].

$\rho_x = \frac{8M}{Na_o^3}$, where *M* is the molecular weight of the sample, *N* is the Avogadro's number and a_o is the lattice constant.

The porosity *P* of the nano-ferrites was determined using the relation.

$$P = 1 - \frac{\rho_b}{\rho_x}$$

The X-ray diffraction data is further used to calculate the tetrahedral and octahedral ionic radii (r_A, r_B) sites, the bond lengths on tetrahedral *(A-O)* and octahedral (*B-O*) sites of cubic spinel structure by using Standely's equations [13].

$$r_A = \left(u - \frac{1}{4}\right)a\sqrt{3} - r\left(O^{2-}\right)$$

$$r_B = \left(\frac{5}{8} - u\right)a - r\left(O^{2-}\right)$$

$$A - O = \left(u - \frac{1}{4}\right)a\sqrt{3}$$

$B - O = \left(\frac{5}{8} - u\right)a$, where *a* is the lattice constant; $r(O^{2-})$ is the radius of oxygen ion (1.35 Å); *u* is the oxygen ion parameter, for ideal spinel ferrite *u=3/8*. Hopping lengths in tetrahedral sites (L_A) and in octahedral sites (L_B) which is nothing but the distance between the magnetic ions, have been calculated using the following relation,

$$L_A = a\left(\frac{\sqrt{3}}{4}\right)$$

$$L_B = a\left(\frac{\sqrt{2}}{4}\right)$$

The magnetic moment (μ_B) has been calculated from the hysteresis data by using the relation [14]

$$\mu_B = \frac{Molecular\ \ weight \times Saturation\ magnetization}{5585}$$

The Y-K angles have been calculated using the relation

$$\mu_B = 5(1+x)\cos\alpha_{YK} - 5(1-x)$$

III. Result And Discussion

3.1 XRD analysis

Fig.1. shows the XRD patterns of $Co_{1-x}Zn_xFe_2O_4$ ($x=0.2, 0.4, 0.6, 0.8$) samples at sintering temperatures *200ºC* and *400ºC*. The diffraction patterns exhibit six reflection planes (220), (311), (400), (422), (511), (440). These well-defined reflections without any ambiguity, exhibits the formation of a single phase cubic spinel structure. It can also be noticed that the (hkl) value of the entire peak are unmixed which indicates face centred cubic (fcc) structure. The broad XRD peak for the samples sintered at 200ºC indicates that the ferrite particles are of nano size, whereas sintering brings about increase in grain size giving rise to sharp well defined peaks.

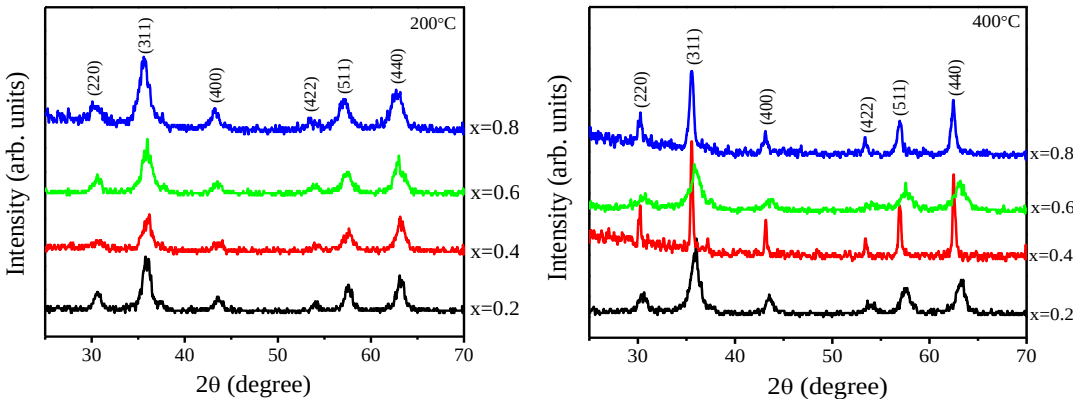

Fig. 1. X-ray diffraction patterns of $Co_{1-x}Zn_xFe_2O_4$ sintered at 200ºC and 400ºC

From the XRD data, the average grain size for each composition has been calculated from the XRD line width of the highest intensity peak (311) using Scherrer formula [15]. The grain size for $Co_{1-x}Zn_xFe_2O_4$ has been found to be within the range of 4 nm- 9 nm. In all cases, the grain size decreases as the zinc content was increased, whereas grain size increases with the increase of sintering temperature. The decrease in grain size can be explained by the particle size effect, more specifically, the effect of surface stress [16]. The precise lattice constant a_o, was determined by plotting lattice parameter versus Nelson-Riley function and using a least square fit method. Lattice constant increases regularly with increase in Zn content (Fig. 2). This behaviour of lattice constant with Zn content *x* is explained on the basis of difference in ionic radii of Zn^{2+} and Co^{2+}. Replacement of larger Zn^{2+} (0.82 Å) cations for smaller Co^{2+} (0.78 Å) cations in the cobalt zinc ferrite causes an increase in lattice constant and decrease in grain size. The values of the grain size and lattice constant for all temperatures as deduced from the X-ray data has been given in the Table 1. It can be concluded that the zinc substitution plays dominant role in influencing the value of lattice constant.

With the change of zinc content and sintering temperature, density also changes. The effect of Zn substitution and sintering temperature on the X-ray density (ρ_x), bulk density (ρ_b) and porosity (P) has been shown in Table 1.

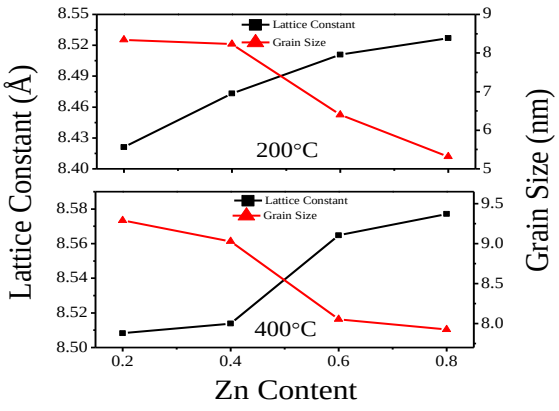

Fig. 2. Variation of lattice constant and grain size

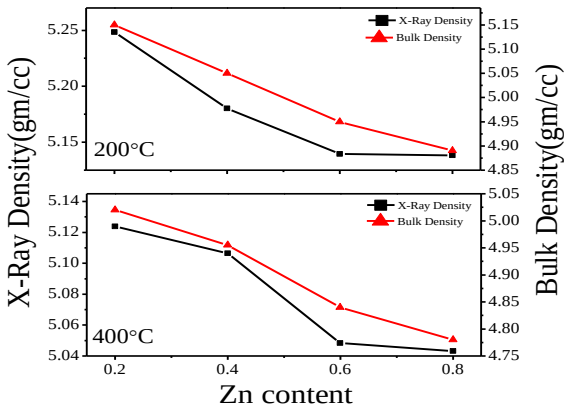

Fig. 3. Variation of X-ray density and bulk density

X-ray density (ρ_x) depends upon the lattice constant and molecular weight. As the lattice constant increases with the increase of Zn concentration and sintering temperature, a corresponding decrease of the X-ray density has been observed. A similar result has been observed by Pandit et al. in Mg-Zn ferrite [17]. It is also observed that X-ray densities are higher in magnitude than the corresponding bulk densities. This may be due to the existence of pores which were formed and developed during the sample preparation or the sintering process [18]. This increase in X-ray density is also due to the difference in ionic radii between Co and Zn [19]. It can be seen from Table 1 that the X-Ray density lies in the range of 5.25 gm/cm^3 to 5.04 gm/cm^3. Fig. 3 shows the effect of Zn content on the X-ray density (ρ_x) and bulk density (ρ_b) of the samples. It is observed that bulk density also decreases with the increase in Zn content. The decrease in densities can be ascribed to the density of Zn^{2+} (7.14 gm/cm^3), which are lower than those of Co^{2+} (8.9 gm/cm^3) and Fe^{3+} (7.86 gm/cm^3) [20]. Other than the difference in specific density of the constituent ions, the bulk densities are also governed by the porosities of the sintered sample. The porosity values are found to increase significantly with increasing Zn content. The composition $x= 0.2$ has the highest X-ray density, bulk density and lowest porosity for all temperatures. This increase in porosity and decrease in density are due to the increase in lattice constant because the grains may be of irregular shape [18]. During the sintering process, the discontinuous grain growth takes place. The inter-granular porosity is increased due to discontinuous grain growth [21].

Table 1

Different parameters estimated from XRD for $Co_{1-x}Zn_xFe_2O_4$

Sintering Temp. (ºC)	Zn^{2+} Content x	Lattice Constant Å	Grain Size nm	ρ_x (gm/cc)	ρ_b (gm/cc)	P (%)	r_A Å	r_B Å	A-O Å	B-O Å	L_A Å	L_B Å
200	0.2	8.42	8	5.25	5.15	1.87	0.473	0.755	1.823	2.105	3.646	2.977
	0.4	8.47	8	5.18	5.05	2.51	0.485	0.768	1.835	2.118	3.669	2.996
	0.6	8.51	6	5.14	4.95	3.69	0.493	0.778	1.843	2.128	3.685	3.009
	0.8	8.53	5	5.14	4.89	4.83	0.496	0.782	1.846	2.132	3.692	3.015
400	0.2	8.51	9	5.12	5.02	2.03	0.492	0.777	1.842	2.127	3.684	3.008
	0.4	8.51	9	5.11	4.96	2.96	0.493	0.778	1.843	2.128	3.687	3.010
	0.6	8.56	8	5.05	4.84	4.13	0.504	0.791	1.854	2.141	3.709	3.028
	0.8	8.58	8	5.04	4.78	5.22	0.507	0.794	1.857	2.144	3.714	3.032

The mean ionic radius of the tetrahedral (A) "r_A" and octahedral (B) "r_B" site was calculated, the values have been also listed in Table 1 for all samples. It can be seen that the bond lengths (A-O, B-O) and ionic radii (r_A, r_B) increase with increasing the zinc content as well as sintering temperature, which in turn causes an increase in the lattice constant. In fact, the mean tetrahedral ionic radius shows slow increase than that of the ionic radius of octahedral site with increasing the content of zinc. Similar findings on the Co-Zn system have been reported by other investigators [22]. The hopping lengths in the tetrahedral site (L_A) and in octahedral site (L_B) which is nothing but the distance between the magnetic ions have been calculated and the values have also been given in Table 1. It is seen that distance between the magnetic ions increases as the zinc content and sintering temperature increases.

3.2 Measurement of magnetization

Fig. 4 shows the plots of magnetization (M) as a function of applied magnetic field (H). Table 2 lists different parameters like saturation magnetization (M_s), remanent magnetization (M_r), the ratio of remanent magnetization to saturation magnetization (M_r/M_s), coercivity, magnetic moment (μ_B), Yafet-Kittel angles α_{YK} and Curie temperature (T_C).

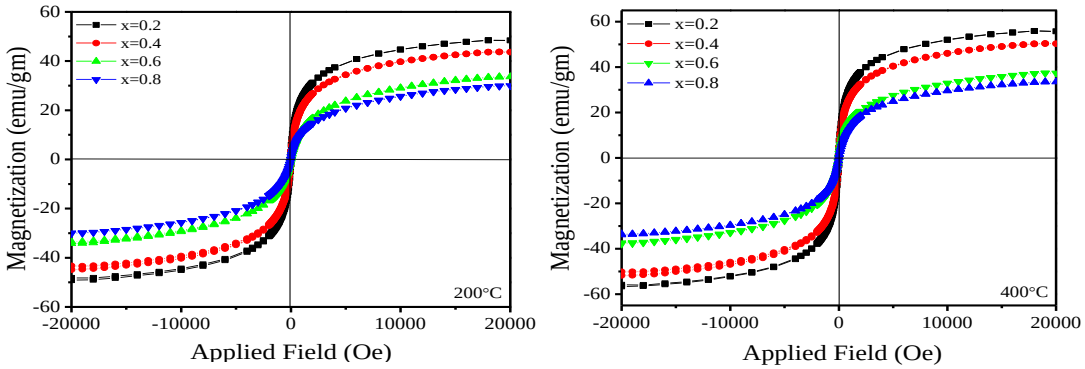

Fig. 4. Hysteresis loops of $Co_{1-x}Zn_xFe_2O_4$ sintered at 200ºC and

It is seen that the magnetic properties change with the increase of zinc content *x* and sintering temperature. The parameter M_s, M_r, M_r/M_s and μ_B decrease with increase in *x*. The decrease in these values results from the existence of spin canting, which has been reported in several nanometer sized ferrites [23]. In a cubic system of ferromagnetic spinels, the magnetic order is mainly explained on the basis of cation distribution and super exchange interaction mechanism occurring between iron and cobalt ions between the metal ion at tetrahedral A and octahedral B sites. The substitution of non-magnetic ion such as zinc, which has a preferentially A site occupancy results in the reduction of the exchange interaction between A and B sites, resulting in strengthening of B-B interaction. When Zn^{2+} ions are introduced at the expense of cobalt ions, some of the Fe^{3+} ions migrate from A to the B sites in view of the site preferences for different ions. This increases the Fe^{3+} ion concentration at B-sites. As Zn^{2+} concentration increases, the iron ions left at A-site, being small in number, the A-B interaction experienced by B-site iron ions decreases. Also, the increased number of Fe^{3+} ions at the B-site increases the B-B interaction, resulting in spin canting [24]. The low values of M_r/M_s ratio indicate an appreciable fraction of supermagnetic particles. M_r/M_s decreases to 0.00 indicating a fraction of the particles in the blocked state.

From the Table 2, it is observed that coercivity decreases with increasing Zn^{2+} content. Fig. 5 also shows the variation of M_S and coercivity with zinc content for 200ºC and 400ºC. This is due to its direct relationship with anisotropy constant of the sample. The anisotropy constant decreases with increasing Zn^{2+} content, which in turn decreases the domain wall energy [25, 26].

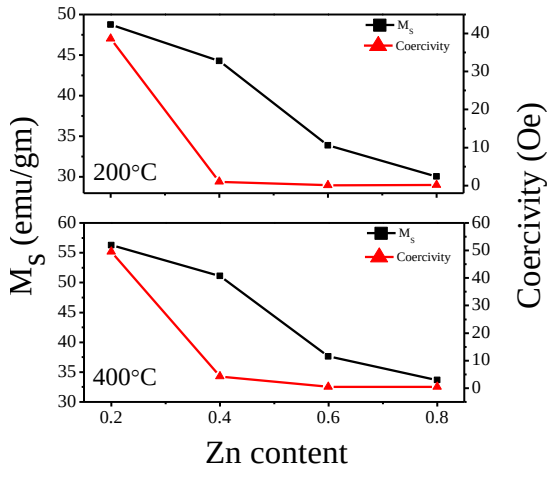

Fig. 5. Variation of saturation magnetization and coercivity

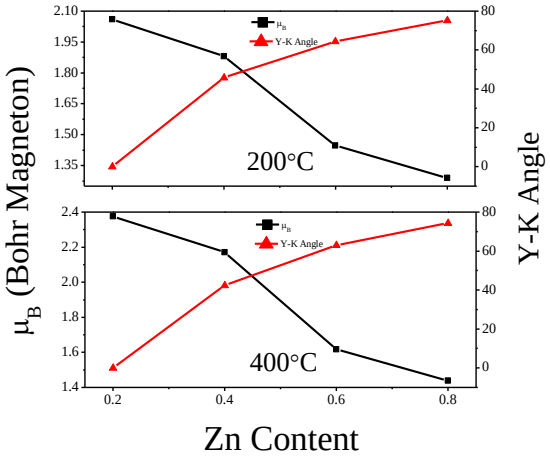

Fig. 6. Variation of magnetic moment and Y-K angle with Zn content

The variation of magnetic moment and Y-K angles with Zn^{2+} content has been shown in Fig. 6. Y-K angles [27] increases due to the existence of canted spins comparing the strength of A-B and B-B super exchange interaction. The Nielsen's [28] three-sublattice model is predominant for this rise.

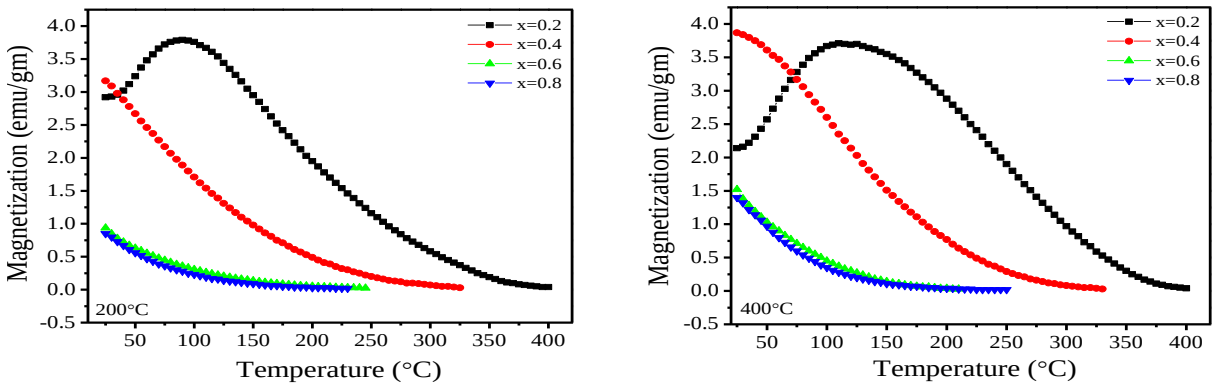

Fig. 7. Variation of magnetization with temperature sintered at 200ºC and 400ºC

From Fig. 7, it can be seen that magnetization decreases very slowly with the increase of temperature. From the graph, Curie temperature for all compositions has been determined. Curie point indicates the degree of homogeneity in the sample composition [29]. The linear decrease of T_C with increasing *Zn* content for sintering temperature 200ºC and 400ºC has been shown in Fig. 8. This may be explained by modification of the A-B exchange interaction strength due to the change of the cation distribution between A and B sites when non-magnetic *Zn* is substituted for *Co*. A similar trend in the variation of T_C has been observed by some workers in *Mg-Zn* [30] and *Li-Zn* [31] ferrites.

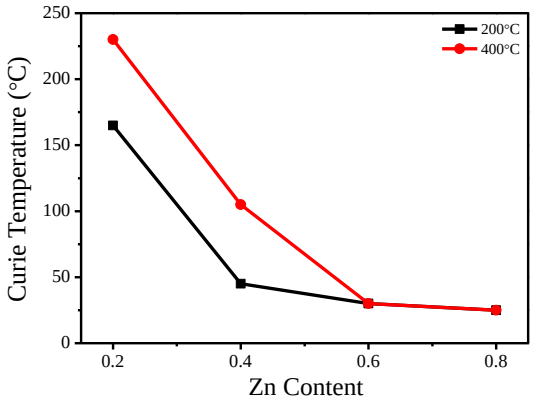

Fig. 8. Variation of Curie temperature with Zn content

Table 2

Magnetization data of $Co_{1-x}Zn_xFe_2O_4$

Temp. (ºC)	Zn^{2+} Content, *x*	M_S (emu/gm)	M_r (emu/gm)	M_r/M_S	Coercivity (Oe)	μ_B (Bohr magneton)	Y-K Angle (α_{YK})	Curie Temp. (ºC)
200	0.2	48.77	2.55	0.05	38.65	2.06	0	165
	0.4	44.30	0.07	0.00	1.05	1.88	45.80	45
	0.6	33.90	0.00	0.00	0.08	1.45	64.45	30
	0.8	30.04	0.00	0.00	0.13	1.29	75.26	25
400	0.2	56.26	3.74	0.07	49.58	2.38	0	230
	0.4	51.11	0.41	0.01	4.21	2.17	42.39	105
	0.6	37.65	0.01	0.00	0.46	1.62	63.10	30
	0.8	33.67	0.02	0.00	0.47	1.44	74.27	25

IV. Conclusion

Wet chemical co-precipitation method has been employed to synthesize $Co_{1-x}Zn_xFe_2O_4$ ferrite samples at nanometer scale. The Ferrites have been sintered at 200ºC and 400ºC for three hours. The presence of *Zn* ions causes appreciable changes in the structural and magnetic properties of the $Co_{1-x}Zn_xFe_2O_4$ ferrite. The X-ray diffraction studies clearly showed the formation of single phase spinel structure and the grain size within nano-

scale. In addition, the average grain size has been found to increase with the sintering temperature, while it decreases with the increase of zinc content. The lattice constant and porosity also increases, while the X-ray density and bulk density shows a decreasing behaviour with increasing Zn content. The lattice constant is found to increase from 8.42 Å to 8.58Å with increasing zinc content and sintering temperature. This change is due to the larger ionic radius of Zn^{2+} (0.82 Å) compared with that of Co^{2+} (0.78 Å). Whereas, the grain size decreases from 9 nm to 5 nm on increasing zinc content. The saturation magnetization, remanent magnetization, coercivity and magnetic moment have been found to show a decreasing behavior, while Y-K angle show increasing behaviour with the increase of Zn content. As revealed by the observed results, the magnetic properties of the samples are mainly dominated by Zn^{2+} non magnetic ions replacing Co^{2+} ions as well as migration of Fe^{3+} ions from octahedral to tetrahedral sites. Low field hysteresis loop shows a decreasing trend in corecivity with Zn contents due to increased magnetic softness. All the coercivity values were sufficiently low to confirm that the ferrite was a soft ferrite. Experimental data shows that sintering temperature has great influence on the Curie temperature. It is also seen that the Curie temperature decreases with the increase of Zn content, while it is increases with the increase of sintering temperature. All experimental data reveals that the zinc substitution plays a key role to change its structural and magnetic properties significantly.

Acknowledgment

The authors are thankful to Materials Science Division, Atomic Energy Centre, Dhaka-1000, Bangladesh for supporting experimental facilities.

References

[1]. Y. N. Xia, P. Yang, Y. Sun, Y. Wu, B. Mayers, B. Gates, Y. Yin, F. Kim and H. Yan, "One dimensional nanostructures: synthesis, characterization and applications", *Adv. Mater.* 15, 2003, 353.
[2]. X. Kou, F. Xin, H. Zhu, Q. J. Xiao, "Tunable ferromagnetic resonance in *NiFe* nanowires with strong magnetostatic interaction", *Appl. Phys. Lett.* 94, 2009, 112509.
[3]. Q. A. Pankhurst, N. K. T. Thanh, S. K. Jones and J. Dobson, "Progress in applications of magnetic nanoferrites in biomedicine", *J. Phys. D: Appl. Phys.* 42, 2009, 224001.
[4]. C. C. Berry, "Progress in functionalization of magnetic nanoferrites for applications in biomedicine", *J. Phys. D: Appl. Phys.* 42, 2009, 224003.
[5]. Santosh Bhukal, Tsering Namgyal, S. Mor, S. Bansaland Sonal Singhal, "Structural, electrical, optical and magnetic properties of chromium substituted Co-Zn nanoferrites $Co_{0.6}Zn_{0.4}Cr_xFe_{2-x}O_4$ ($0 \le x \le 1.0$) prepared via sol-gel auto-combustion method", *J. Mol. Structure*, 1012, 2012, 162-167.
[6]. D. S. Mathew and R. S. Juang, "An Overview of Structure and Magnetism of Spinel Ferrite Nanoferrites and their Synthesis in Microemulsions", *Journal of Chemical Engineering*, 129 (1-3), 2007, 51-65.
[7]. B. W. Samaila, H. Mansor, "Sintering temperature dependence of room temperature magnetic and dielectric properties of $Co_{0.5}Zn_{0.5}Fe_2O_4$ prepared using mechanically alloyed nanoferrites", *J. Magn. Magn. Mater.*322, 2010, 686–691.
[8]. S. Dey and J. Ghose, "Synthesis, Characterization and Magnetic Studies on Nanocrystalline $Co_{0.2}Zn_{0.8}Fe_2O_4$", *Materials Research Bulletin*, 38 (11-12), 2003, 1653-1660.
[9]. R. Arulmurugan, B. Jeyadevan, G. Vaidyanathan and S. Sendhilnathan, "Effect of Zinc Substitution on Co-Zn and Mn-Zn Ferrite Nanoferrites Prepared by Co-Precipitation", *J. Magn. Magn. Mater.*, 288, 2005, 470-477.
[10]. M. U. Islam, M. U. Rana and T. Abbbas, "Study of Magnetic Interactions in Co-Zn-Fe-O System", J. *Mat. Chem. and Phy.*, 57 (2), 1998, 190- 193.
[11]. G. Vaidyanathan, S. Sendhilnathan, R. Arulmurgan, "Structural and Magnetic Properties of $Co_{1-x}Zn_xFe_2O_4$ Nanoferrites by Co-Precipitation Method", *J. Magn. Magn. Mater.*, 313 (2), 2007, 293-299.
[12]. A. M. M. Ferea, S. Kumar, K. M. Batoo, A. Yousef, C. G. Lee, Alimuddin, "Structure and electrical properties of $Co_{0.5}Cd_xFe_{2.5-x}O_4$ Ferrites", *J. Alloy Compound*, 464, 2008, 361-369.
[13]. J. Standely, Oxide Magnetic Materials, Clarendon, Oxford, UK, 1972.
[14]. L. Vegard, "Die Konstitution der Mischkristalle und die Raumfüllung der atome", *Zeits Phys.*5, 1921, 17–26.
[15]. R. Arulmurugan, B. Jeyadevan, G. Vaidyanathan and S. Sendhilnathan, "Effect of Zinc Substitution on Co-Zn and Mn-Zn Ferrite Nanoferrites Prepared by Co-Precipitation", *J. Magn. Magn. Mater.*, 288, 2005, 470-477.
[16]. F. J. Owens and C. P. Poole, *The Physics and Chemistry of Nanosolids*, New Jersey: John Wiley & Sons, Inc., 2008.
[17]. A. Pandit, A. R. Shitre, D. R. Shengule, K. M. Jadhav, "Magnetic and dielectric properties of $Mg_{1-x}Mn_xFe_{2-2x}O_4$ ferritesystem", *J. Mater. Sci.* 40, 2005, 423–428.
[18]. Muhammad, A. Maqsood, "Structural, electrical and magnetic properties of $Cu_{1-}xZnxFe_2O_4$ ferrites ($0 \le x \le 1$)", *J. Alloy. Com.*. 460, 2008, 54–59.
[19]. T. Abbas, M. U. Islam, M. Ashraf Ch, "Study of sintering behavior and electrical properties of Cu-Zn-Fe-O system", *Modern Phys. Lett. B.*9, 1995, 1419–1426.
[20]. J. Smit, H. P. J. Wign, *Ferrites*. Wiley, New York, 1959.
[21]. A. Verma, O. P. Thakur, C. Prakash, TC. Geol, R. G. Mendirth, "Temperature dependence of electrical properties of nickel-zinc ferrites processed by the citrate precursor technique", *Mater Sci. Eng. B.* 116, 2005, 1–6.
[22]. N. M. Deraz and A. Alarifi, *J. Anal. Appl. Pyrolysis*, 2011.
[23]. E. Berkowitz, W. J. Scuele, P. J. Flanders, *J. Appl. Phys.* 39(2), 1969, 1261.
[24]. S. E. Shirsath, B. G. Toksha, R. H. Kadam, S. M. Patange, D. R. Mane, G. S. Jangam and A. Ghasemi, "Doping Effect of Mn^{2+} on the Magnetic Behavior in Ni-Zn Ferrite Nanoferrites Prepared by Sol-Gel Auto-Combustion", *J. Phy. Chem. Sol.*, 71 (12), 2010, 1669-1675.
[25]. Y. M. Yakovlev, E. V. Rubalikaya and N. Lapovok, "Ferromagnetic Resonance in Lithium Ferrite", *Soviet Physics Solid State*, 10, 1969, 2301-2303.
[26]. H. K. Jun, J. H. Koo and T. J. Lee, "Study of Zn-Ti Based H_2S Removal Sorbents Promoted Co and Ni Oxides", *Energy Fuels*, 18 (1), 2004, 41-48.

[27]. Z. C. Xu, "Magnetic anisotropy and Mossbauer spectra in disordered lithium-zinc ferrites", *J. Appl. Phys.* 93, 2003, 4746–4749.
[28]. *Magn. Magn. Mater.* 324, 2012, 2116–2120.
[29]. T. Nakamura, T. Miyamoto and Y. Yamada, "Complex Permeability Spectra of Polycrystalline Li-Zn Ferrite and Application to EM-Wave Absorber", *J. Magn. Magn. Mater.*, 256 (1-3), 2003, 340-347.
[30]. S. Noor, M. A. Hakim, S. S. Sikder, S. M. Hoque, K. H. Maria, P. Nordblad, "Magnetic behaviour of Cd^{2+} substituted cobalt ferrites", *J. Phys. Chem. Solids* 73, 2012, 227–231.
[31]. S. Akhter, M.A. Hakim, "Magnetic properties of cadmium substituted lithium ferrites". *J. of Mater. Chem. Phys.* 120, 2010, 399–403.